

HIGH GRADIENT PERFORMANCE OF X-BAND ACCELERATING SECTIONS FOR LINEAR COLLIDERS

T. HIGO, T. TANIUCHI, M. YAMAMOTO, J. ODAGIRI,
S. TOKUMOTO, H. MIZUNO and K. TAKATA

*KEK, National Laboratory for High Energy Physics,
1-1, Oho, Tsukuba, Ibaraki, 305 Japan*

I. WILSON and W. WUENSCH

CERN, 1211 Geneve 23, Switzerland

(Received 1 March 1994; in final form 5 July 1994)

The KEK high gradient test facility is described. Results are given of tests made on two 22-cell TW sections – one ‘KEK’ made by Japanese industry and the other ‘CERN’ made using technology developed for CLIC. The KEK structure was conditioned to an average accelerating gradient E_{av} of 68 MV/m in 600 hours. The CERN structure reached 85 MV/m (a peak field level of 138 MV/m) in 50 hours – these fields were limited by the power available from the klystron. The dark current at 50 MV/m was less than a few μA for the CERN section but 20 to 30 μA for the KEK section.

KEY WORDS: Linear collider, radio-frequency devices

1 INTRODUCTION

The feasibility of building a high energy electron-positron linear collider using high-frequency accelerating structures is being studied at CERN, INP (Protvino), KEK and SLAC. The basic philosophy behind the high-frequency approach is as follows. The linacs should be as short as possible to minimise the capital cost. For a given beam energy this means high accelerating gradients. High frequencies are used to transfer RF power to the beam very efficiently and reduce wall plug power. The end result is that a short high frequency high gradient linac has an overall wall plug power consumption which is comparable with other approaches. The main disadvantage of high frequencies is increased transverse wakefields and as a direct result tighter alignment tolerances. Accelerating fields of 50 to 100 MV/m at X-band in travelling wave (TW) accelerating sections are being considered for JLC,¹ whereas CLIC has chosen to operate at 80 MV/m at 30 GHz.² These

field levels are well beyond the performance of present day accelerators and experimental studies are required to demonstrate that they can be achieved at these frequencies.

This report describes an X-band high gradient test facility that was built at KEK, and gives results of tests made on two 22-cell TW sections – one ‘KEK’ made by Japanese industry and the other ‘CERN’ made using technology developed for CLIC. Similar experiments on X-band structures are also being carried out at SLAC.³

2 ACCELERATING SECTIONS

The KEK and CERN structures have almost the same electrical design. Each structure has 20 regular cells with 2 coupler cells and is operated in $2\pi/3$ mode at 11.4 GHz. The calculated structure parameters are summarized in Table 1. The difference in group velocity comes from a small difference in the rounding of the coupling irises. A constant impedance structure was chosen to avoid complicating the dark current production mechanism by field emitted electrons hitting smaller downstream irises. The cross sections of the two structures are shown in Figure 1 and a photo of one of the structures in Figure 2.

The couplers of the two structures are slightly different. The input and output waveguide irises are 2 mm thick and rounded for the CERN section and 0.5 mm thick with sharp edges for the KEK section. The input and output waveguide height is reduced by a uniform taper for CERN and by a quarter wave step for KEK. The corresponding beam-pipe lengths for the two sections are 19.3 mm and 9.8 mm.

KEK cells were machined on a precision lathe to a typical surface roughness of $0.2\ \mu\text{m}$ from C1011 copper supplied by Furukawa Electric Co, Japan. The cells were cleaned using

TABLE 1: Design Parameters of the accelerating structures.

Geometry	Param	KEK	CERN	[unit]
Beam hole radius	a	3	3	[mm]
Disk thickness	t	2	2	[mm]
Effective length (22 cells)	L	0.1924	0.1924	[m]
Group velocity	v/c	0.01177	0.0111	
Impedance	R'/Q	15.74	16.0	[k Ω /m]
Shunt impedance	r	103.6	106.8	[M Ω /m]
Q- value	Q	6584	6680	
Attenuation parameter	α	1.545	1.615	[neper/m]
Total attenuation	$\tau=\alpha L$	0.297	0.311	[neper]
Filling time	t_f	55	58	[ns]
Surface field enhancement	E_p/E_{acc}	3.91/2	3.91/2	

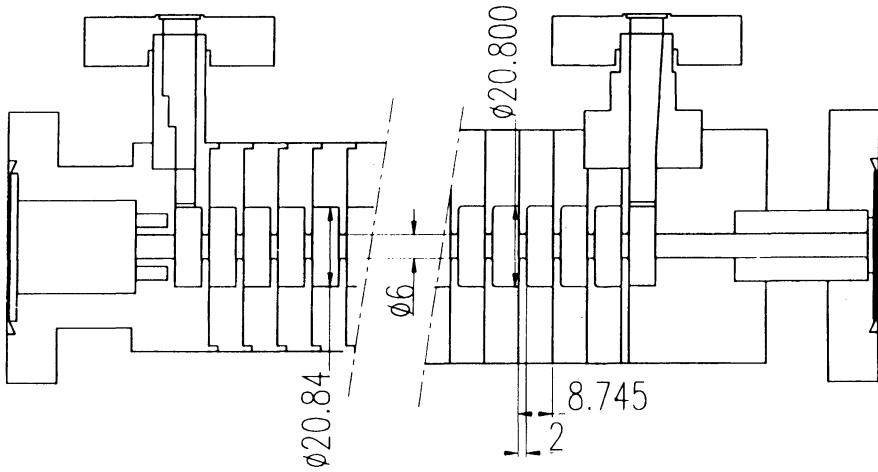


FIGURE 1: The main geometrical features of the two accelerating sections (KEK on the left, and CERN on the right)

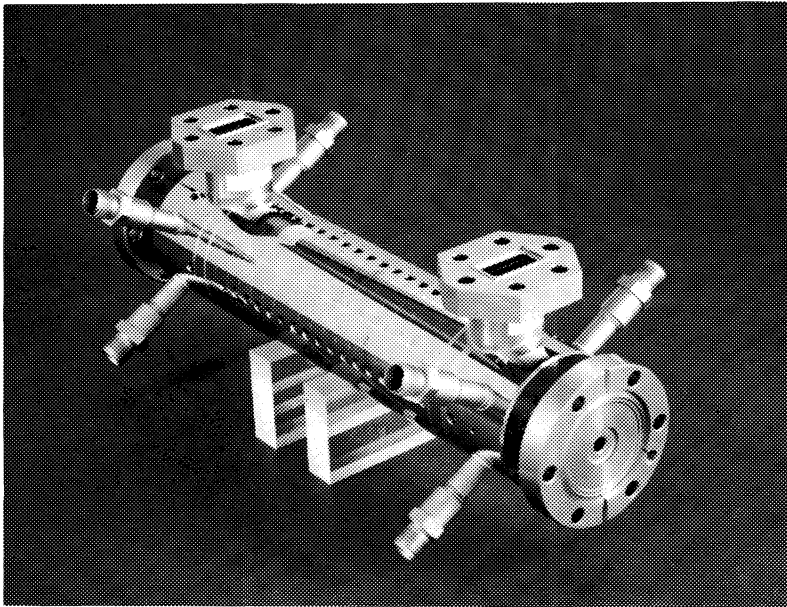


FIGURE 2: The CERN accelerating section

the normal cleaning process for commercial vacuum components and were then brazed in a hydrogen furnace. Gold braze was used for the couplers and silver braze for the regular cells. The couplers were matched by both dimple-tuning of the outer wall of the coupler cell

and mechanical deformation of the waveguide iris. The section was then tuned by dimpling the outer walls of individual cells according to the standard on-axis detuning rod technique. The detuning rod was allowed to sit and probably even slide on the irises during this process.

CERN cells were machined on an ultra-precision lathe (Rank-Pneumo MSG 325) to a typical surface roughness of $0.02 \mu\text{m}$ from C101 copper supplied by Outokumpu, Finland. They were cleaned using CERN's standard procedure for copper vacuum components and brazed in a vacuum furnace. All joints were made with a silver braze. The section including the coupler cells was tuned by dimpling the outer walls of individual cells. The detuning rod was not allowed to touch the irises during this process.

Both sections were assembled and tuned in a normal laboratory environment (not in clean rooms).

3 WORKING FORMULAE

Input power and peak accelerating field are related by

$$E_{\text{in}}[\text{MV/m}] = 18.6\sqrt{P_{\text{in}}[\text{MW}]}.$$

The accelerating field averaged over the full length of a structure, E_{av} , for a flat power pulse (non-SLED), is defined as

$$\begin{aligned} E_{\text{av, flat}} &= E_{\text{in}}[1 - \exp(-\tau)]/\tau \\ &= 0.86E_{\text{in}} \end{aligned}$$

For the SLED system, which does not give a flat output pulse but rather an exponential decay (see Figure 5), the integrated field along the structure becomes maximum when the head of the RF pulse reaches the output coupler. The average field is then given by

$$E_{\text{av, SLED}} = 0.616E_{\text{in}, t=0}$$

where $E_{\text{in}, t=0}$ is the unattenuated peak field of the SLED pulse in the structure.

The output dark current from the structure was analysed using the modified Fowler–Nordheim (FN) formula⁴

$$\frac{I_f}{E_s^{2.5}} = C \exp\left(\frac{-6.53 \cdot 10^9 \varphi^{1.5}}{\beta E_s}\right)$$

where I_f is the field emission current, C a constant, φ the work function for Cu (4.5 eV) and β the field enhancement factor. It is unclear whether the peak or average surface field should be used for E_s in the expression above – the field enhancement factor β varies in any case by less than 15%.

Dark current is defined to be the current occurring *during* the RF pulse and is calculated from the average Faraday cup current / (pulse length \times repetition rate).

TABLE 2: Distance from input (output) coupler cell to the measuring device.

Device	Distance (mm)	Aperture (mm)
Upstream current transformer	100	\varnothing 16
Upstream Faraday cup	430	\varnothing 36
Profile monitor	150	\varnothing 36
Downstream current transformer	300	\varnothing 16
Analyser magnet	660	24 \times 24
Downstream Faraday cup	1130	\varnothing 36

4 EXPERIMENTAL SETUP AND INSTRUMENTATION

The set-up is shown in Figure 3(a). The structure, vacuum equipment and all measuring devices were mounted on a common platform [see Figure 3(b)] and were shielded with one meter thick concrete blocks.

The RF power was generated by an XB-50K klystron⁵ and transported to the structures through a 5.5 m long rectangular waveguide. For the final stage conditioning of the CERN structure, a SLED RF pulse compression system was added.

The input, reflected and transmitted RF pulses were monitored through crossguide directional couplers. The coupling was about 60 dB with a directivity better than 23 dB. They were located 60 cm from the structure. The RF signals were detected outside the shielded enclosure by Shottky diodes via 5 m long low-loss cables.

Upstream and downstream average dark currents were measured by Faraday cups (see Table 2). The time structure of the dark current was measured using current transformers (see Table 2). The winding ratio was 10:1, the response time was better than one ns, and the droop over 100 ns was negligible. The output was monitored by an oscilloscope.

The transverse profile of the dark current was monitored with a 1.2 mm thick luminescent alumina ceramic plate doped with chromium oxide. It was mounted downstream of the structure at an angle of 45° with respect to the structure axis and was monitored by a TV camera.

The downstream dark current momentum spectrum was measured using a dipole analyzer magnet and a Faraday cup. The 20 mm thick stainless-steel plates separated by 10 mm gave a momentum acceptance of 4.3%.

Five cylindrical plastic scintillators, 8 mm diameter and 20 mm long, were equally spaced along the structure between the input and output couplers. The scintillators looked at the structure through 12 mm diameter holes in lead shielding blocks. The distance between the cavity centre axis and the scintillators was about 5 cm. The light from the scintillator was guided through an 8 mm diameter, 1.5 m long light guide to a photomultiplier and the output monitored by an oscilloscope.

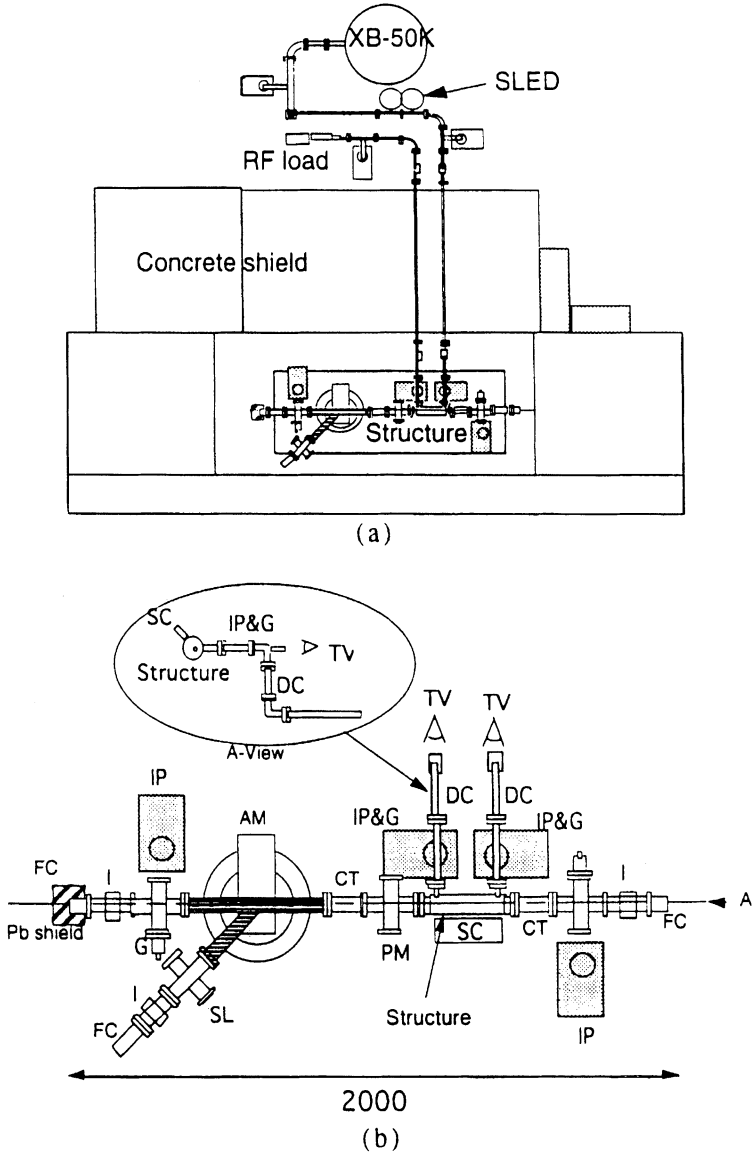


FIGURE 3: Experimental setup. (a): Klystron, SLED, structure, RF load, etc. (b): setup in detail; CT: current transformer, FC: Faraday cup, AM: analyser magnet, SL: slits, I: insulating duct, SC: scintillation counter, DC: directional coupler, PM: profile monitor, IP: ion pump, G: cold cathode gauge, TV: TV monitor.

TABLE 3: Conductances of various components in the vacuum system.

Aperture	Dimension [mm]	Conductance [l/s]
Cell to cell	\varnothing 6 every 8.75	2.4 (for 1 cell)
Input/output waveguide iris	$5 \times 7.5 \times 0.5$	4
Waveguide to ion pump	\varnothing 1.5 \times 36	10
Waveguide	22.86×10.12	0.6 (for 1 m)
Cut-off beam pipe (KEK)	\varnothing 6 \times 9.8 long	1.3
Cut-off beam pipe (CERN)	\varnothing 6 \times 19.3 long	0.7
Beam line	\varnothing 36	5.2 (for 1 m)

The structure was pumped by four 20 l/s ion pumps through the two coupler irises and the beam pipes as shown in Figure 3(b). Vacuum levels were monitored by cold cathode gauges. Because most high frequency components have small transverse dimensions vacuum conductances are also small (see Table 3). The vacuum level in the coupler is estimated to be about 5 times larger than that measured at the waveguide pumping port.

Conditioning was automatically controlled by a VAX3500 through a CAMAC system. The RF power level was varied by changing the applied voltage to the klystron and was interlocked to both reflected power and vacuum levels.

5 EXPERIMENTAL RESULTS

The KEK and CERN structures were conditioned for most of the time with 50 ns and 100 ns long pulses respectively at a repetition rate of 50 Hz. The RF power level to the structure was slowly ramped up until either a reflected power or vacuum interlock was activated. The vacuum interlock threshold was set at 10^{-4} Pa. The reflected RF interlock threshold was adjusted as conditioning progressed to be just above the normal non-break-down level.

Typical RF pulse shapes and current transformer outputs are shown in Figure 4. The two peaks in the reflected signal occur because the high frequency components of the steeply rising and falling edges of the RF pulse are outside the bandwidth of the structure. The RF pulse for SLED operation is shown in Figure 5.

E_{av} versus number of shots for both structures is shown in Figure 6. For the KEK structure, 600 hours conditioning with 6×10^7 shots were needed to reach the maximum field of 68 MV/m. Frequent breakdowns in the final 100 hours of conditioning prevented any further increase in field level. A particularly difficult power barrier was encountered around the 55–60 MV/m level after 3×10^7 shots (see points marked by crosses in Figure 6).

The maximum field of 85 MV/m was obtained for the CERN structure in only 50 hours and less than 1×10^7 shots. This field level was only limited by the available power from the klystron and SLED pulse compression system.

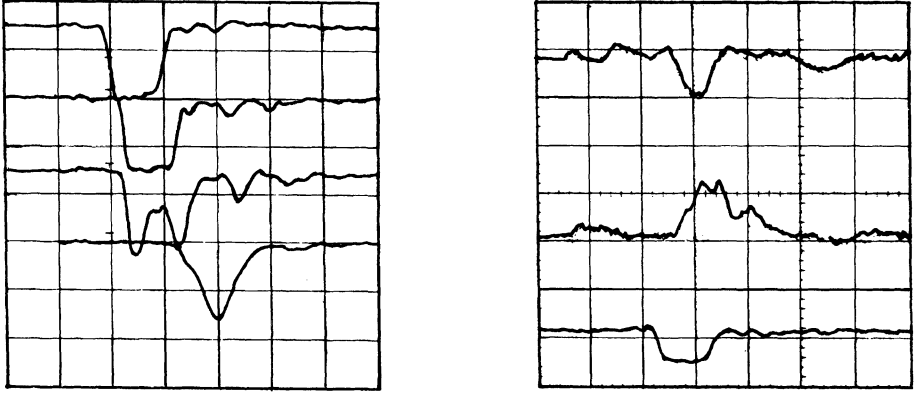


FIGURE 4: (Left) Typical klystron output, structure input, reflected and transmitted signals (from top to bottom) (Right) Typical upstream and downstream current transformer outputs, and RF input for the KEK section. The time-scale is 50 ns/div.

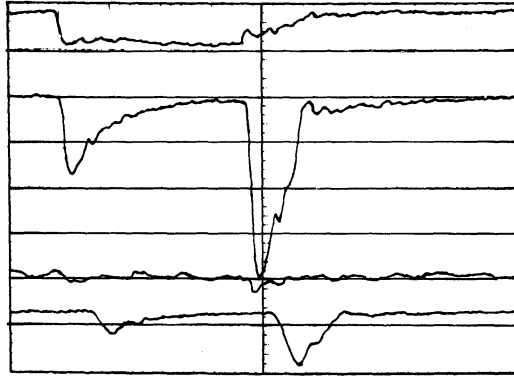
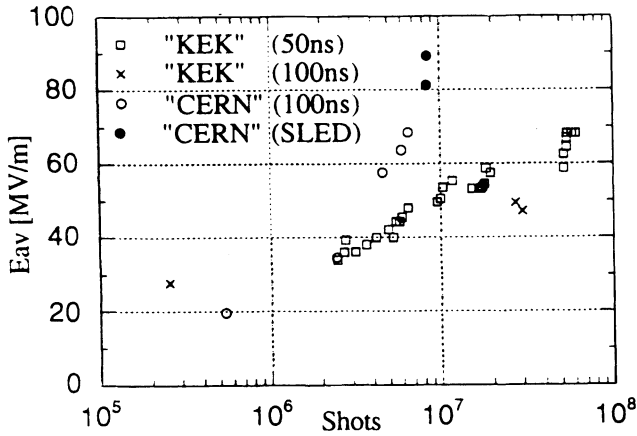
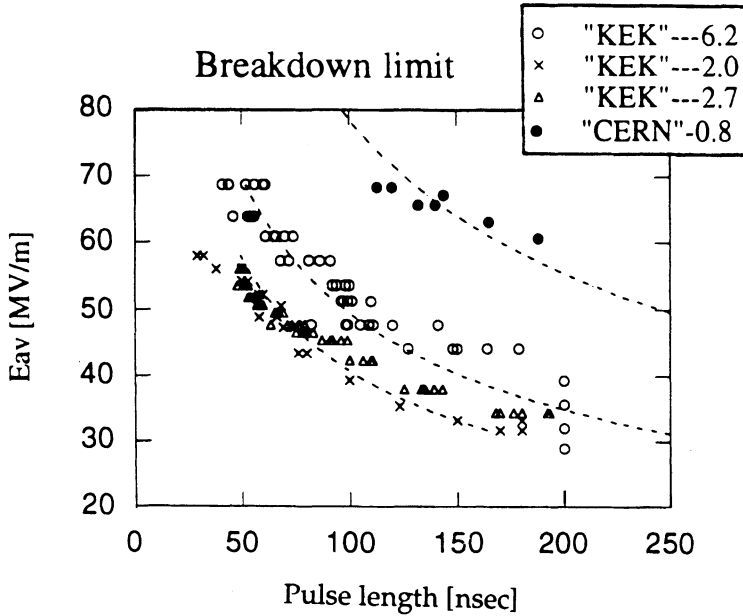


FIGURE 5: Typical SLED operation. Traces are klystron output, SLED output pulse, reflected and transmitted signals (from top to bottom). The time-scale is 100 ns/div.

The breakdown limit as a function of pulse length at various stages of conditioning for the KEK structure, and for the CERN structure at the final stage of non-SLED conditioning are shown in Figure 7. The data can be reasonably fitted by a $t^{-1/2}$ dependence.

Almost all the breakdowns of both structures had one of two types of reflected power signatures: an increased amplitude reflection of the same duration as the input pulse or an increased length reflection. Examples of the two types are shown in Figure 8.

The base vacuum level was rather stable during conditioning although a rapidly increasing field level caused occasional increases of the vacuum level by almost an order of magnitude. The base vacuum levels at the waveguide of the input coupler, at the waveguide of the output coupler and at the beam line were 1.3×10^{-5} , 0.6×10^{-5} and 0.2×10^{-5} (Pa) respectively.

FIGURE 6: E_{av} versus number of shots for both structures.FIGURE 7: Breakdown field versus pulse length. Numbers to the right of the symbols are the number of shots in units of 10^7 . The dotted lines show a $t^{-1/2}$ dependence.

The increase of the vacuum level with the RF on was very small. The base vacuum level was therefore determined by the outgassing rate without RF and the pumping speed. The estimated maximum vacuum level inside the structure was about 1.0×10^{-4} Pa at the input coupler cell.

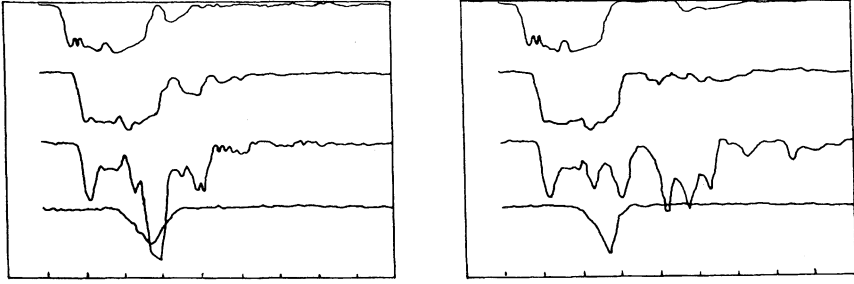


FIGURE 8: The two characteristic types of RF breakdowns. The time-scale is 50 ns/div. The traces are (from top to bottom) klystron output, structure input, reflected and transmitted signals.

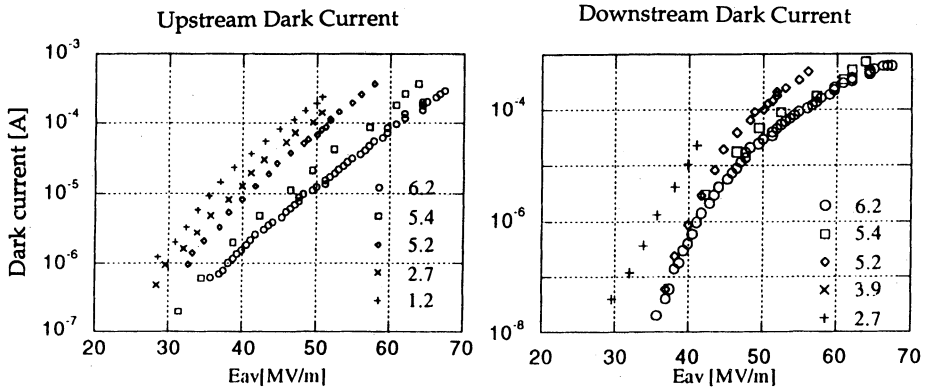


FIGURE 9: Dark current versus E_{av} for the KEK structure for 50 ns long pulses. Numbers to the right of the symbols are the number of shots in units of 10^7 .

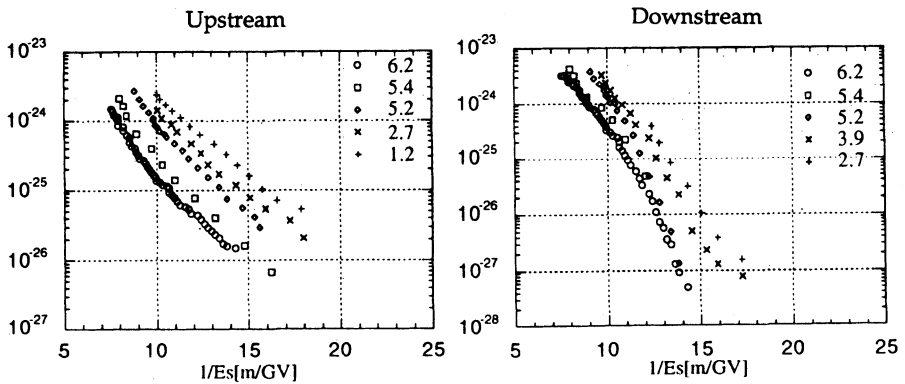


FIGURE 10: Modified Fowler-Norheim plots at various stages of conditioning of the KEK structure. Numbers to the right of the symbols are the number of shots in units of 10^7 .

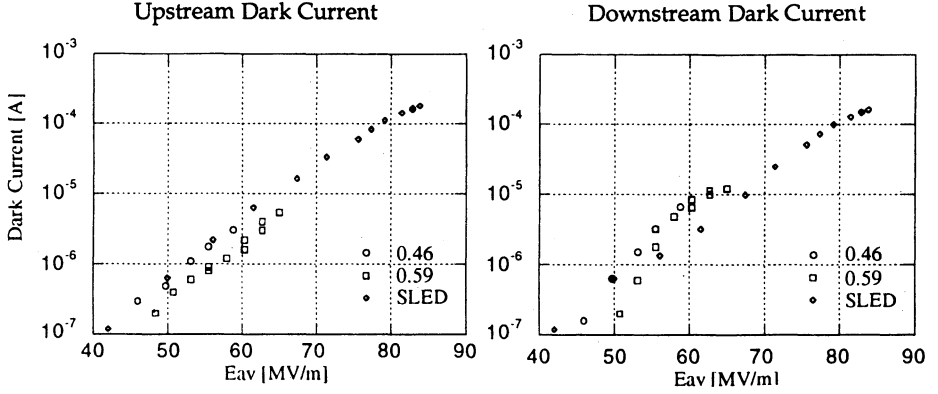


FIGURE 11: Dark current versus E_{av} for the CERN structure for 100 ns long pulses (for non-SLED). Numbers to the right of the symbols are the number of shots in units of 10^7 .

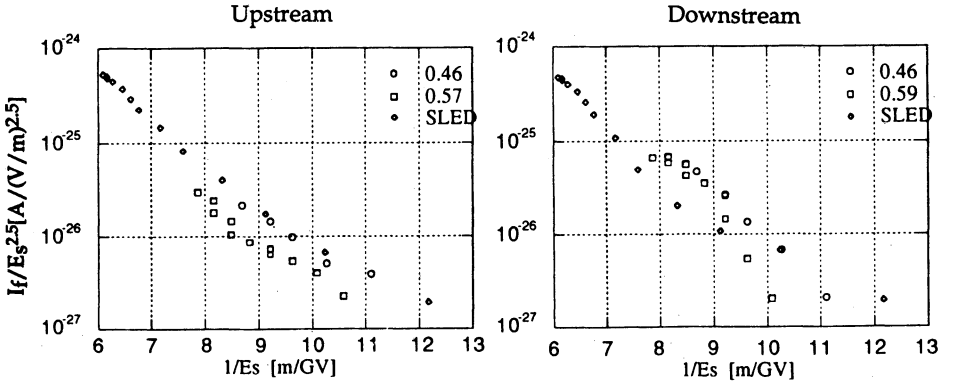


FIGURE 12: Modified Fowler-Norheim plots at various stages of conditioning of the CERN structure for 100 ns long pulses (for non-SLED). Numbers to the right of the symbols are the number of shots in units of 10^7 .

Plots of dark current versus E_{av} for both structures at various stages of conditioning are shown in Figs. 9 and 11. Both the upstream and downstream dark current of the KEK structure decreased monotonically by more than an order of magnitude during conditioning.

Figures 10 and 12 show the data in modified Fowler-Nordheim plots. The upstream data show a linear behaviour. The downstream data show a change of slope at $E_{av}=35$ to 50 MV/m for the KEK structure and 60 MV/m for the CERN structure with a reduced field enhancement factor at higher fields. This feature is probably related to the onset of dark current capture. For an electron starting from rest, the analytically derived value for the capture field is 61 MV/m⁶.

The dark current generated in the KEK structure with an accelerating gradient of 50 MV/m at various stages of conditioning is shown in Figure 13. The dark current decreased even

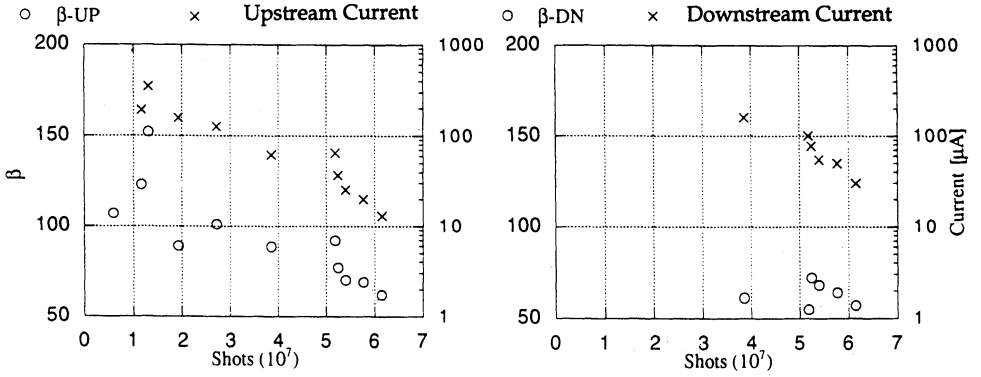


FIGURE 13: Field enhancement factor and dark current at $E_{av} = 50$ MV/m as a function of conditioning of the KEK structure for 50 ns pulses.

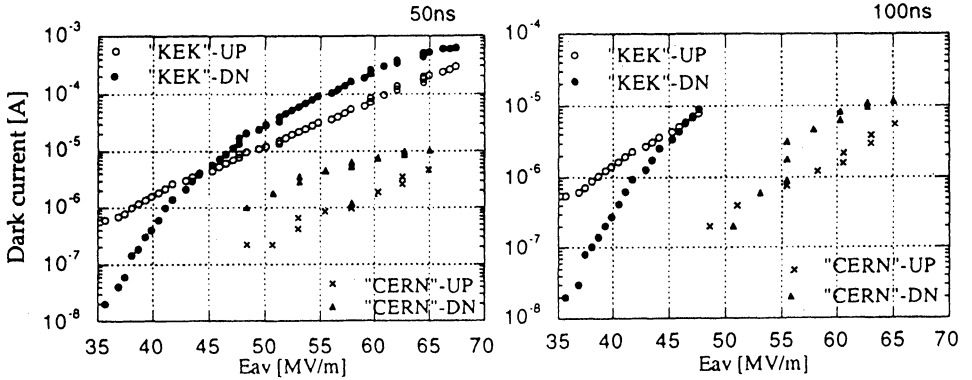


FIGURE 14: Dark current versus E_{av} for both structures for 50 and 100nsec pulses at the final stage of conditioning (before pulse compression).

when the maximum field had ceased to improve (see the last three points in Figures 13 and 6). Field enhancement factors β -up and β -down reached values around 50 to 60 and are also shown in Figure 13.

Dark current as a function of E_{av} at the final stage of conditioning for both structures are shown in Figure 14. At 50 MV/m and a pulse length of 50 ns the dark current of the KEK structure was more than 10 times larger than that of the CERN structure. With a pulse length of 100 ns the ratio increased to over 100. The KEK structure was frequently breaking down at 50 MV/m and 100 ns which may explain the disproportionately high level of dark current. Modified Fowler–Nordheim plots are shown in Figure 15.

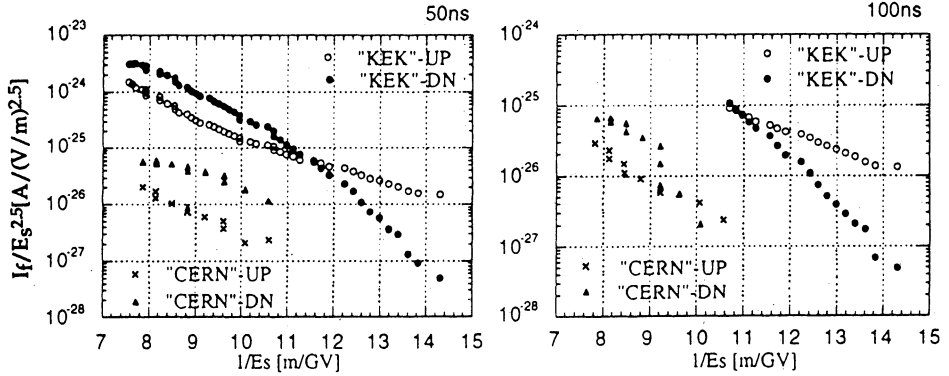


FIGURE 15: Modified Fowler-Nordheim plots for both structures for 50 and 100 ns pulses at the final stage of conditioning (before pulse compression).

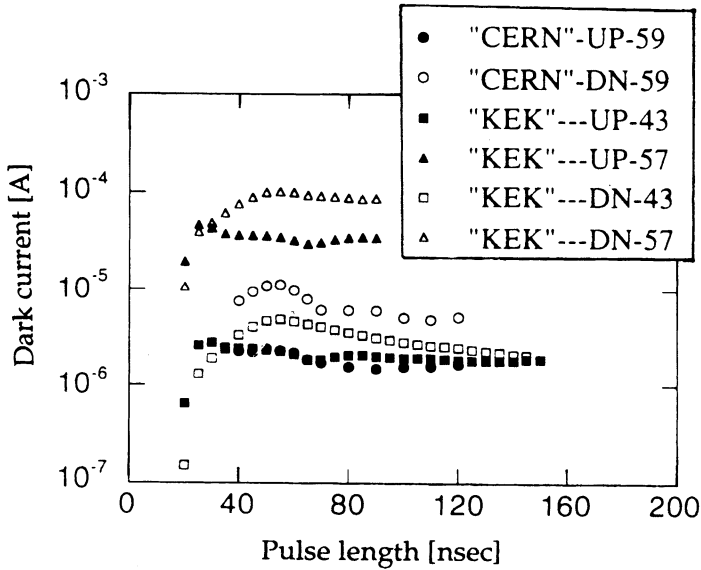


FIGURE 16: Dark current versus pulse length. The numbers in the symbol definitions are E_{av} in MV/m.

Peak current versus pulse width is shown in Figure 16. Upstream dark current is roughly constant for pulse widths longer than 25 ns. This result suggests that this current comes mainly from the input coupler region and is continuously created during an entire pulse. The downstream current increased with pulse length up to one filling time and decreased thereafter. One would expect constant dark current above one filling time when the full length of the section contributes to the trapping process. The decrease for longer pulses can

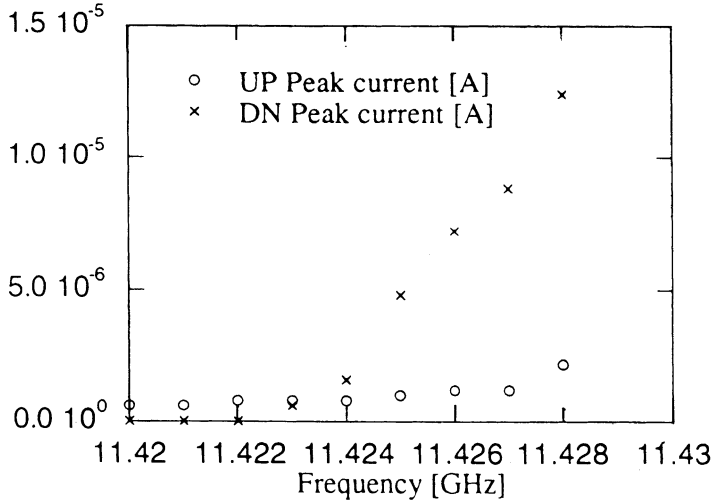


FIGURE 17: Dark current versus operating frequency for the CERN structure at $E_{av}=59$ MV/m.

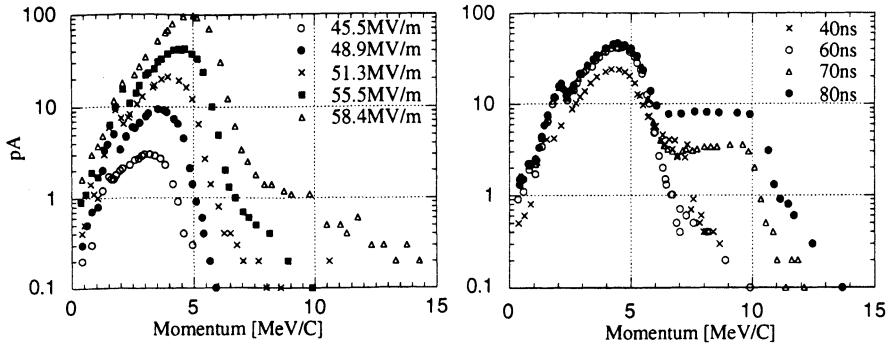


FIGURE 18: Dark current energy spectra of the KEK structure for (a) 60 ns long pulses with varying E_{av} , (b) $E_{av} = 56$ MV/m and varying pulse lengths.

be explained by the decreasing relative contribution of the high frequency components of the rising and falling edges (see the section on frequency dependence of dark current). As the pulse length is reduced below one filling time, the length over which trapping occurs is reduced and the level of dark current falls. The data indicate that for very short pulses the higher dark current yield caused by the increased relative contribution of the high frequency components does not compensate for this decrease in trapping length.

Dark current versus operating frequency is plotted in Figure 17. Little or no change in upstream current was measured. The downstream dark current increased as the π mode was approached. This phenomenon is the same as that observed at SLAC³.

Momentum spectra of the dark current from the KEK structure are shown in Figure 18. All the spectra went through a maximum between 3–5 MeV/c. As the pulse length was

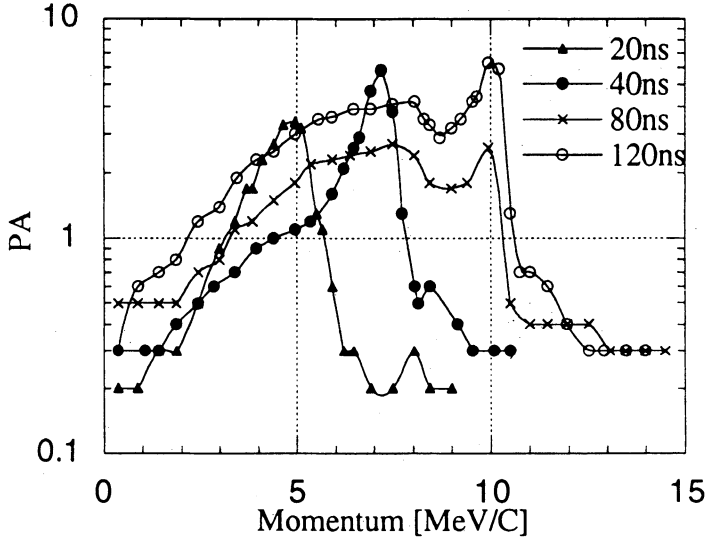


FIGURE 19: Dark current energy spectra of the CERN structure for 59 MV/m and varying pulse lengths.

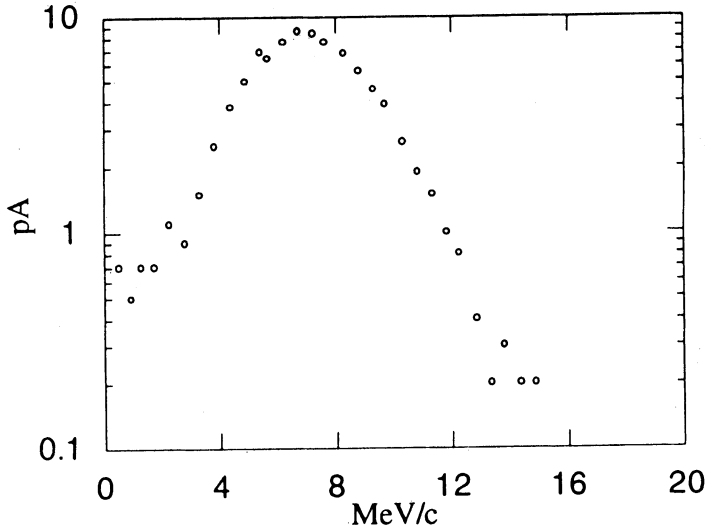


FIGURE 20: Dark current energy spectra of the CERN structure for $E_{av} = 72$ MV/m using pulse compression by SLED.

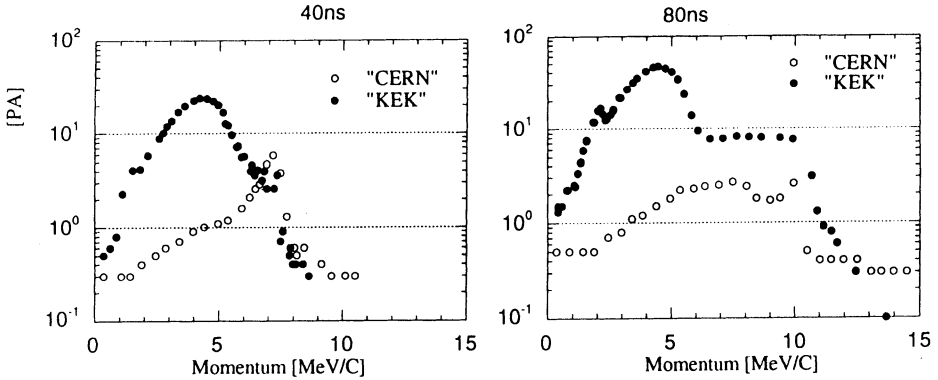


FIGURE 21: Dark current energy spectra for the two structures for 40 ns pulses (below a filling time) and 80ns (above a filling time). E_{av} was 56 MV/m for the KEK section and 59 MV/m for the CERN section.

increased above a fill time, a plateau emerged with a maximum energy cut-off corresponding to acceleration by the entire structure. Momentum spectra of the dark current from CERN are shown in Figure 19 for various pulse lengths. The spectral change with pulse length is complex. The momentum spectrum with SLED in operation is shown in Figure 20. The end point of the spectrum is in agreement with the full acceleration. The momentum spectra for both structures are compared in Figure 21. A large amount of low energy dark current was observed in the KEK case but not in the CERN case.

6 CONCLUSIONS AND COMMENTS

Since the two structures differ only slightly in geometry – in the input and output couplers – the higher field levels obtained and the reduction in dark current are probably due to differences in the two fabrication techniques. Noteworthy points are that the CERN structure has a much better surface finish, was cleaned differently, was brazed in vacuum instead of hydrogen, has no braze inside the cells and the detuning rod for dimple tuning did not touch the irises.

This work has demonstrated that the field levels required for X-band linear colliders are feasible. Extrapolating the results to 30 GHz it is expected that operation at the nominal CLIC gradient of 80 MV/m will be even less of a problem since both the tendency to spark and the level of dark current will decrease as the frequency is increased and the pulse length is shortened. It is expected that full-length (1.3 m) X-band structures would attain the same maximum gradient but would require proportionally more conditioning time. Simulations⁷ show that the level of dark current increases exponentially as the number of cells is increased up to a maximum (around 30 cells) and thereafter remains constant. There is no well-defined criterion for the maximum acceptable level of dark current, the level will depend on the wakefields, the beam position monitor signals and the power losses that the dark current induces, and the relative importance given to these effects will vary from one machine design to another.

REFERENCES

1. JLC Group, 'JLC-I', KEK-Report 92-16, December 1992.
2. W. Schnell, 'The CERN Study of a Linear Collider in the TeV Range', CERN SL/91-49, December 1991.
3. J. Wang, *et al.*, 'High-gradient studies on 11.4 GHz copper accelerator structures', 16th Int. Linac conference, Ottawa, August 1992.
4. G.A. Loew and J.W. Wang, 'RF Breakdown Studies in Room Temperature Electron Linac Structures', XIII Int. Symposium on Discharges and Electrical Insulation in Vacuum, Paris, France, 1988, SLAC-PUB-4647, 1988 and references therein.
5. H. Mizuno, *et al.*, 'X-band Klystron for Japan Linear Collider', KEK Preprint 90-90, 1990.
6. P.M. Lapostolle and A.L. Septier, Linear Accelerators, North-Holland, Amsterdam 1970.
7. S. Yamaguchi, 'Simulation studies on high-gradient experiments', LAL / RT 92-18 December 1992.